Journal of Photochemistry & Photobiology, B: Biology 226 (2022) 112370

Contents lists available at ScienceDirect

Journal of Photochemistry & Photobiology, B: Biology

journal homepage: www.elsevier.com/locate/jphotobiol

Effects of free radicals from doxycycline hyclate and minocycline hydrochloride under blue light irradiation on the deactivation of *Staphylococcus aureus*, including a methicillin-resistant strain

Jeu-Ming P. Yuann [a], Shwu-Yuan Lee [b], Sin He [a], Tak-Wah Wong [c], Meei-Ju Yang [d], Chien-Wei Cheng [a], Shiuh-Tsuen Huang [e,f,**], Ji-Yuan Liang [a,*]

[a] Department of Biotechnology, Ming Chuan University, Gui Shan 333321, Taiwan
[b] Department of Tourism and Leisure, Hsing Wu University, New Taipei City 244012, Taiwan
[c] Department of Dermatology, National Cheng Kung University Hospital, Department of Biochemistry and Molecular Biology, College of Medicine, Center of Applied Nanomedicine, National Cheng Kung University, Tainan 70101, Taiwan
[d] Tea Research and Extension Station, Yangmei 326011, Taiwan
[e] Department of Science Education and Application, National Taichung University of Education, Taichung 40306, Taiwan
[f] Department of Soil and Environmental Sciences, National Chung Hsing University, Taichung 40200, Taiwan

ARTICLE INFO

Keywords:
Blue light
Doxycycline
Minocycline
MRSA
Staphylococcus aureus

ABSTRACT

Doxycycline hyclate (DCH) and minocycline hydrochloride (MH) are tetracycline antibiotics and broad-spectrum antimicrobial agents. The changes in DCH and MH under blue light (λ = 462 nm) irradiation in alkaline conditions (BLIA) were investigated. Deactivation caused by superoxide anion radical ($O_2^{\bullet-}$) and deactivation from DCH and MH during photolysis on *Staphylococcus aureus* (*S. aureus*), including methicillin-resistant *S. aureus* (MRSA), were studied. DCH is relatively unstable compared to MH under BLIA. The level of $O_2^{\bullet-}$ generated from the MH-treated photoreaction is lower than that from DCH photolysis, and the DCH-treated photoreaction is more efficient at inactivating *S. aureus* and MRSA at the same radiant intensity. DCH subjected to BLIA decreased the viability of *S. aureus* and MRSA by 3.84 and 5.15 log, respectively. Two photolytic products of DCH (PPDs) were generated under BLIA. The mass spectra of the PPDs featured molecular ions at *m/z* 460.8 and 458.8. The molecular formulas of the PPDs were $C_{21}H_{22}N_2O_{10}$ and $C_{22}H_{24}N_2O_9$, and their exact masses were 462.44 and 460.44 g/mol, respectively. These results bolster the photolytic oxidation that leads to DCH-enhanced deactivation of *S. aureus* and MRSA. Photochemical treatment of DCH could be applied as a supplement in hygienic processes.

1. Introduction

Tetracyclines (TCs) belonging to a group of broad-spectrum antibiotics interfere with aminoacyl-tRNA binding to the bacterial ribosome and inhibit protein synthesis in microorganisms [1]. TCs are extensively applied as antibiotics in the clinic and as subtherapeutic growth promoters to prevent animal diseases [2]. TCs are formed from tetracyclic nuclei, which are composed of various functional groups attached to the nucleus, such as chlortetracycline, demeclocycline, doxycycline hyclate (DCH), minocycline hydrochloride (MH), oxytetracycline and tetracycline (TC). Many functional groups that are attached to tetracyclic nuclei change their molecular properties and affect their antibiotic ability.

Staphylococcus aureus (*S. aureus*) is often detected in the respiratory tract or skin of humans and results in a broad scope of poisons and symptoms of disease [3], which are also known as skin and soft tissue infections (SSTIs) and accompanied by a broad range of clinical infections, such as cellulitis or necrotizing fasciitis. The aetiology of acute SSTIs is often aerobic *β-haemolytic streptococci* and *S. aureus* infection [4]. In 2012, after investigating isolates from 163 medical centres in the US, the surveillance programme of Assessing Worldwide Antimicrobial Resistance Evaluation (AWARE) determined that *S. aureus*, *Escherichia coli* (*E. coli*) and *Klebsiella* spp. are the most commonly distinguished

; MRSA, methicillin-resistant *Staphylococcus aureus*.

* Corresponding author.
** Corresponding author at: Department of Science Education and Application, National Taichung University of Education, Taichung 40306, Taiwan.
E-mail addresses: hstsuen@mail.ntcu.edu.tw (S.-T. Huang), liang121@mail.mcu.edu.tw (J.-Y. Liang).

https://doi.org/10.1016/j.jphotobiol.2021.112370
Received 4 June 2021; Received in revised form 16 November 2021; Accepted 24 November 2021
Available online 27 November 2021

bacteria, with respective incidence rates of 55.5, 5.9 and 5.5 [4]. *S. aureus* is also one of the most important pathogens for hospital-acquired infection and is related to fatal illnesses, such as bacteremia, endocarditis and pneumonia [5].

The adaptability of *S. aureus* has led to widespread epidemics in humans, and numerous attempts to contain the spread of *S. aureus* have had unsatisfactory results. Transfer of antibiotic resistance genes among different *staphylococcal* strains is the main cause. Methicillin-resistant *S. aureus* (MRSA) carries the *mec*A gene encoding penicillin-binding protein 2a (PBP2a), a transcriptase with a weak affinity for β-lactam antibiotics, including penicillin and methicillin, which allows bacterial cell wall synthesis in the presence of methicillin [6]. In addition, this strain develops resistance to a majority of other common antimicrobial agents [7]. MRSA was discovered in 1961 shortly after the introduction of methicillin [8]. As a virulent pathogen, MRSA is responsible for diseases with onset in both healthcare and community settings [9]. Globally, antimicrobial resistance has been a major health concern among human and veterinary medications [10]. Vancomycin is usually reserved to treat MRSA infections. Unfortunately, vancomycin-resistant *S aureus* (VRSA) strains have been isolated globally since 2001 [11]. A new strategy to surmount drug-resistant *S. aureus* is urgently needed for healthcare providers.

The antibacterial photodynamic inactivation of bacteria (aPDI) is an efficient method for overcoming resistance to bacteria [12,13] because it does not depend on the mode of bacterial resistance. aPDI is an alternative treatment to SSTIs clinically to reduce nosocomial skin infections caused by multi-resistant bacteria [14–17]. Additionally, aPDI causes cell death by producing reactive oxygen species (ROS). ROS, e.g., hydroxyl radicals, singlet oxygen, superoxide anion radicals ($O_2^{\bullet-}$) and peroxyl radicals, are reactive oxygen-containing molecules or free radicals [18–20]. $O_2^{\bullet-}$ is an intermediate generated by redox reactions. In a previous study, the inactivation of *E. coli*, *S. aureus* and MRSA was achieved by ROS-induced DNA cleavage generated during the photolysis of riboflavin [18,21,22].

The phototoxicity of TCs is a notable side effect for patients and may be caused by the production of ROS [23]. TC is not stable and is highly sensitive to UVA illumination [24]. ROS are generated via TC photolysis under illumination by simulated sunlight [25]. The photolysis of chlortetracycline [26], demeclocycline [27,28], doxycycline [27,28], oxytetracycline [28], and tetracycline [27,29] deactivates *E. coli* after UV light illumination. Huang et al. showed that $O_2^{\bullet-}$ is produced by TC under BLIA, which increased the aPDI efficacy of gram-negative *E. coli* and multidrug-resistant *E. coli* [30]. Under UV or visible light illumination, longer wavelength illumination with less energy is safe for cells.

DCH and MH are tetracycline antibiotics used to treat many infections, and they are the most often prescribed TCs for the treatment of acne vulgaris [16]. DCH and MH have four-ring structures at positions five, six and seven, as shown in Fig. 1. The structural modification of TCs changes their properties. DCH has dose-related phototoxicity to sunlight, while MH shows insignificant photosensitivity [16]. Among the phototoxic responses after the treatment of pharmaceutical substances, skin irritation after UV and visible light exposure may occur following the formation of ROS in the skin, thus leading to oxidative stress to DNA, lipids and proteins [31]. The photosensitization of DCH or MH by visible light illumination and the generation of $O_2^{\bullet-}$ is worthy of further study to examine the role of ROS from DCH or NH photolysis in the enhancement of the bacterial inactivation profile by a photolytic reaction.

The process of aPDI working through either type I ($O_2^{\bullet-}$, •OH) or type II (singlet oxygen, $^1O_2$) photoreaction depends on the photosensitizer used during irradiation [32]. Consistent with previous studies [30,33–35], $O_2^{\bullet-}$ from the TC photoreaction is deemed important to the kinetics of TC photodegradation. Extremely low quantum (Φ_Δ) values, which were lower than 0.03 for $^1O_2$ generation by TCs upon direct photoirradiation, were barely noticed even in the most favourable cases [36]. The superoxide anion ($O_2^{\bullet-}$) was extensively found in TC aqueous solution upon exposure to white light, although the generation of $O_2^{\bullet-}$ was dependent on the specific absorption wavelength of TC [33,34]. Electron spin resonance (ESR) spectrometry and ROS scavenging experiments demonstrated that TC photolysis was involved in $O_2^{\bullet-}$-mediated self-sensitized photolysis [35]. Reports indicated the lack of an appreciable TEMP-$^1O_2$ signal detected in TC solution under light irradiation, while the six peaks characteristic of the DMPO-$O_2^{\bullet-}$ spin adduct were detected, suggesting that $O_2^{\bullet-}$ (but not $^1O_2$) was the species generated upon irradiation of TC in solution [35]. Therefore, in terms of bacterial inactivation due to ROS from DCH and MH photoreaction, $O_2^{\bullet-}$ is the major species produced by direct photolysis in this study.

Antimicrobial control of infections in humans and animals is a worldwide health issue. The evolution of new antibiotics often takes decades. DCH or MH can cause degradation of bacteria after illumination with blue light, while little is known about this photodegradation process. This study determines the effects of blue light photolysis of DCH or MH on the inactivation of *S. aureus* and MRSA via the generation of $O_2^{\bullet-}$. The microbial viability of *S. aureus* and MRSA were used to verify this technique.

2. Materials and Methods

2.1. Photolytic System

The photolytic system for this study was described previously [37,38]. The system consists of a plastic cup that encircled with blue LED strip lights (12 V, VitaLED Company, Tainan, Taiwan) in a container, as shown in Fig. 2. Blue LED strip lights emit a maximum wavelength at 462 nm with a $W_{1/2}$ of 26 nm (spectral peak width at half-height). The reaction solutions were placed in a transparent glass test tube on top of a photoreaction cup. A solar power metre (TM-207, Tenmars Electronics Co., Taipei, Taiwan) and a power supply were used to determine the irradiance of blue light. The plastic cup was maintained at 25 ± 3 °C and monitored by an infrared thermometer (MT 4, Raytek Co., Santa Cruz, CA) during the photolytic reaction.

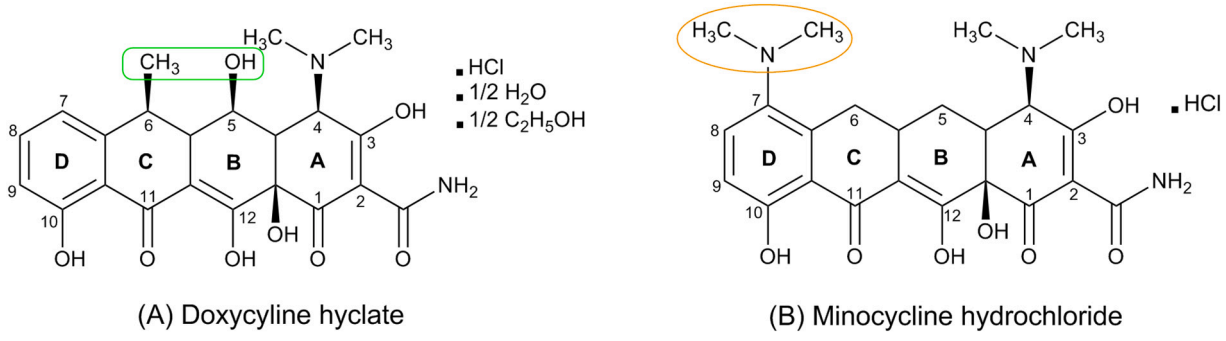

Fig. 1. Chemical structures of (A) doxycycline hyclate (DCH) and (B) minocycline hydrochloride (MH).

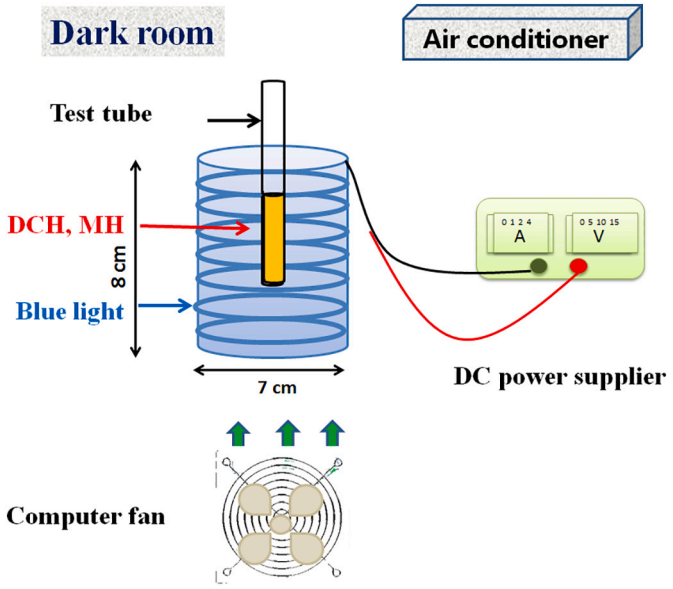

Fig. 2. Photolytic system.

2.2. Chemicals

Doxycycline hyclate (DCH), phenol, *o*-aminophenol, *m*-aminophenol, 3-dimethylaminophenol, L-methionine, *p*-aminophenol, potassium dihydrogen phosphate, potassium hydrogen phosphate and vancomycin (VAN) were purchased from Sigma–Aldrich Co. (St. Louis, MO, USA). Minocycline hydrochloride (MH) was ordered from the Tokyo Chemical Industry Co. (Tokyo, Japan). Nitro blue tetrazolium chloride (NBT) was obtained from Bio Basic Inc. (Markham, Ontario, Canada). The structures of DCH and MH are shown in Fig. 1, and those of the amino phenol compounds are shown in Fig. 3. A Milli-Q system preparation of ultrapure water was used for the solvent throughout this study.

2.3. Blue Light Effects on the Photoreaction of DCH and MH

The blue light effects on DCH and MH photolytic reactions were determined using an ELISA reader (Thermo Fisher Scientific Multiskan, Waltham, MA, USA). DCH or MH (0.1 mM) in 100 mM phosphate buffered solution at pH 7.8 (PB) was left in the dark and used as a control. On the other hand, 0.1 mM DCH or MH was treated with blue light illumination at 2.0 mW/cm^2 in PB (BLIA) for 0.5, 1.0, 1.5, and 2.0 h. The absorbance of DCH or MH after the BLIA treatment was measured from 200 to 800 nm using an ELISA reader.

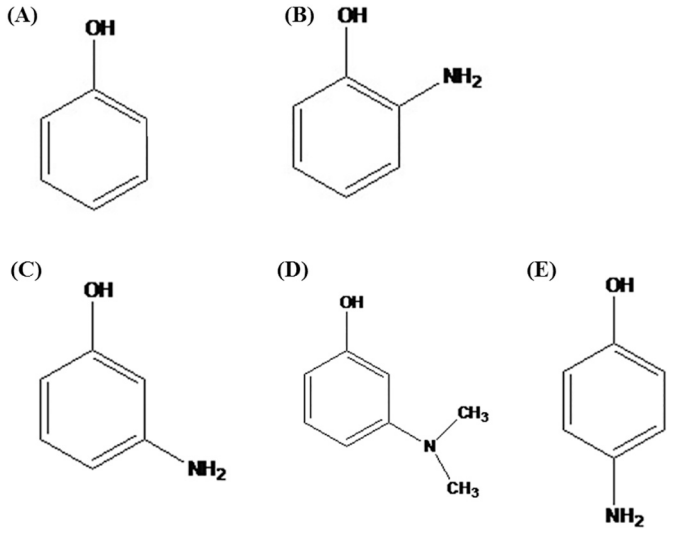

Fig. 3. Chemical structures of (A) phenol, (B) *o*-aminophenol, (C) *m*-aminophenol, (D) 3-dimethylaminophenol and (E) *p*-aminophenol.

2.4. Blue Light Effects on the Photoreaction of Amino Phenol Compounds

Blue light effects on amino phenol compounds, such as phenol, *o*-aminophenol, *m*-aminophenol, 3-dimethylaminophenol and *p*-aminophenol, were determined using an ELISA reader. A 50 mg/L amino phenol compound in PB was left in the dark as a control, while a 50 mg/L amino phenol compound in PB was treated with BLIA for 2 h. The absorbance of the amino phenol compounds treated with BLIA was measured from 200 to 800 nm using an ELISA reader.

2.5. HPLC–MS Assay of DCH Treated with BLIA

The photolytic products of DCH (PPDs) were studied by HPLC–MS analysis, as described previously [39,40]. DCH (0.1 mM) in PB was left in the dark as a control, while 0.1 mM DCH in PB was illuminated with BLIA for 2 h. DCH and PPDs were analysed using the HPLC–MS analytical method. HPLC–MS was performed using an Agilent 1200 series HPLC system connected to an Agilent triple-quadrupole mass spectrometer (6410B, Agilent Technologies, Palo Alto, CA) equipped with an ion source for electrospray ionization (ESI). DCH and PPDs were both detected in negative-ion mode. Nitrogen gas was used as a drying gas with a temperature of 350 °C and a flow rate of 11 L/min, an injection volume of 10 μL, a gas pressure of 50 psi for the nebulizer, a capillary voltage of 3.7 kV, a capillary temperature of 280 °C and m/z = 100–1000. Data were processed using an Agilent MassHunter workstation software (version B.06.00).

Elution of DCH and PPDs was achieved via an Agilent Poroshell 120 EC-C18 threaded column (2.7 μm particle size and 150 mm length × 4.6 mm inner diameter, Agilent Technologies, Palo Alto, CA). Separation was performed by the mobile phase eluent composed of a mixture of methanol (solvent A) and 0.1% formic acid (solvent B), which was eluted at a flow rate of 0.4 mL/min with a ratio profile described in the following. A linear gradient was initiated in intervals of 0–2 min for 5–20% solvent A; 2–8 min for 20% solvent A; 8–12 min for 20–60% solvent A; 12–15 min for 60% solvent A; 15–19 min for 60–95% solvent A; 19–24 min for 95% solvent A; and 24–27 min for 95–5% solvent A. From 27 to 30 min, 5% solvent A was established as the final mobile phase. An injection volume of 10 μL was used for each reaction solution.

2.6. Effects of DCH, MH and VAN on S. aureus and MRSA under Blue Light Illumination

TC under BLIA was used to deactivate gram-negative *E. coli* and a multidrug-resistant bacterium in a previous study [30]. VAN is commonly used for MRSA infections. This study extended the work on DCH, MH and VAN with BLIA to the deactivation of gram-positive *S. aureus* and MRSA.

S. aureus (Taxonomy ID: 10451) from the Bioresource Collection and Research Centre and a clinical isolate of MRSA (Taxonomy ID: JD004) from the National Cheng Kung University Hospital were grown in LB broth at 37 °C overnight. Note that MRSA/JD004 was a single clone isolated from an infected skin wound instead of an epidemic strain. After harvesting, a 0.5 mL culture of *S. aureus* or MRSA/JD004 was placed into a microcentrifuge tube, followed by dilution to an optical density of 0.5 at 600 nm (OD_{600}) (ca. 1.1 × 10^7 CFU/mL).

After 10 min of centrifugation at 10,000 rpm, the supernatant was removed. Then, 1 mL DCH, MH or VAN solution (0.1 mM DCH, MH or VAN in PB) was added. The mixture was placed in a glass tube and treated with BLIA for 2 h. The plate or tube was covered by thick aluminium foil to prevent light illumination for dark control. During the

photolytic reaction, the system was maintained at 25 ± 3 °C. After photolysis, 0.1 mL reactants were diluted, added to plates of LB agar, and incubated overnight at 37 °C. Bacterial survival in subsequent processes was determined by calculating the number of viable colony forming units (CFUs) after overnight growth. Bacterial deactivation was measured by log reduction [= (log (*D*/*B*)], where *B* and *D* are the numbers of CFUs after BLIA [*B*] and the control in the dark [*D*], respectively.

2.7. $O_2^{\bullet-}$ Assay

Both direct and indirect methods can be utilized to detect ROS. The direct method requires special equipment, such as an electron paramagnetic resonance (EPR) spectrometer, while indirect methods are more widely used in biochemical analyses [19]. The nitro blue tetrazolium (NBT) reduction method is an indirect assay for determining the level of $O_2^{\bullet-}$ after NBT is reduced by the $O_2^{\bullet-}$ from intermediates [41]. The effects of DCH and MH under BLIA on the generation of $O_2^{\bullet-}$ were determined by NBT reduction due to the photolytic reaction of riboflavin and FMN. With minor modifications, this protocol was applied as an indicator of $O_2^{\bullet-}$ generation, as previously reported [5,41]. All reagents were prepared prior to the experiments. The chemical L-methionine (0.1093 g) was placed into 75 mL PB, and 0.01 g NBT and 25 mL of either DCH or MH at 0.4 mM were placed into the mixed solution. The respective concentrations of DCH (or MH), methionine and NBT reached 0.1 mM, 7.3 mM and 0.12 mM in the solution. The reaction solution was treated with BLIA for 0.5, 1.0, 1.5, and 2.0 h at room temperature. $O_2^{\bullet-}$ produced from the photolytic process reduces NBT to generate blue formazan that is detectable at 560 nm.

The generation of $O_2^{\bullet-}$ in *S. aureus* from DCH- or MH-treated *S. aureus* subjected to BLIA was determined using the NBT reduction method based on protocols reported previously with minor modifications [42,43]. The sample of the *S. aureus* preparation was basically the same as that described in Section 2.6, except that the 0.5 mL culture of *S. aureus* was placed into a microcentrifuge tube, followed by dilution to an optical density of 0.05 at 600 nm (OD_{600}) (ca. 1.1 × 10^6 CFU/mL). After 10 min of centrifugation at 10,000 rpm, the supernatant was removed. Then, 1 mL of the reaction solution was added. All reagents were prepared prior to the experiments. The chemical L-methionine (0.1093 g) was placed into 75 mL PB, and 0.1 g NBT and 25 mL of either DCH or MH at 0.4 mM were placed into the mixed solution. The concentrations of DCH (or MH), methionine and NBT in the PB solution reached 0.1 mM, 7.3 mM and 1.2 mM, respectively. The mixture was placed in a glass tube and treated with or without BLIA for 2 h. The mixture was centrifuged for 10 min at 10,000 rpm, and then the supernatant was removed. One millilitre of dimethyl sulfoxide *(DMSO)* was added to extract the reduced NBT. Produced from the photolytic process, $O_2^{\bullet-}$ reduces NBT to generate blue formazan that is detectable at 560 nm.

2.8. Statistics

Each test was conducted independently on different days and repeated three times. For each independent experiment, the bacterial sample was subjected to a specific test requirement. The results are expressed as the mean ± standard deviation (SD) of at least three experiments. A homoscedastic two-sample *t*-test was applied to determine whether the means of two populations were different. Statistical significance was set to a $p\ value < 0.05$.

3. Results

3.1. Colour and Spectral Changes in DCH and MH that Are Subjected to BLIA

The photolysis of DCH and MH that is subjected to BLIA was studied.

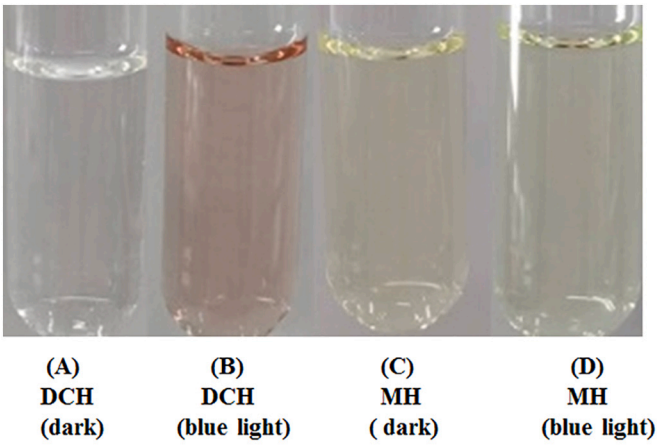

Fig. 4. Colour change in DCH (A, B) and MH (C, D) treated without or with BLIA for 2 h.

Fig. 4B shows that DCH subjected to BLIA turns pink under alkaline conditions (pH 7.8). There was no significant change in colour after exposure to the MH solution and BLIA (Fig. 4D).

Spectral changes in DCH and MH under BLIA are shown in Fig. 5. In the dark, DCH exhibits two major absorptions at 272 and 364 nm. Under BLIA for 0.5–2 h, the photolysis of DCH results in absorption bands with a different profile. DCH is sensitive to blue light, and the absorption at 364 nm is significantly decreased under BLIA. However, for MHs subjected to BLIA for 0.5–2 h, the spectra of the MH solutions are not significantly changed, as shown in Fig. 5 (B). Under blue light irradiation, the degradation rate constants for DCH and MH are shown below.

Niu et al. and Huang et al. reported that the effect of illumination with solar, UV and blue light on TC photolytic kinetics is described by a pseudo-first-order reaction [35,40]. DCH and MH are both tetracycline antibiotics. In Fig. 5, the absorption of DCH or MH at 364 nm is detected after blue light illumination, and the reaction rate for DCH or MH expression is abbreviated as the pseudo-first-order reaction of DCH or MH (Eq. 1). Eq. (2) is the integral of Eq. (1) from $t = 0$ to t = t:

$$-\frac{dC_{DCH}}{dt} = k_{appa} \times C_{DCH} \quad (1)$$

$$-ln\left[\frac{C_{DCH}}{C_0}\right] = k_{appa} \times t \quad (2)$$

where C_0 and C_{DCH} represent the absorbances at t = 0 (initial) and time t for DCH at 364 nm, respectively, while k_{appa} is the rate constant for apparent decomposition. In Fig. 6, the plot of -ln(C/C_0) vs. reaction time produces a linear line with a correlation coefficient (R^2) for DCH subjected to BLIA greater than 0.96; therefore, DCH under BLIA follows pseudo-first-order kinetics in this study. The k_{appa} values for DCH and MH that are subjected to BLIA are 0.1978 and 0.0336 (h^{-1}), respectively, as shown in Fig. 6. The higher k_{appa} value during the DCH photoreaction is ascribed to its photosensitive efficiency under blue light.

3.2. $O_2^{\bullet-}$ Detection by DCH and MH that Are Subjected to BLIA

The generation of $O_2^{\bullet-}$ from the DCH and MH that is subjected to BLIA is determined using the NBT reduction method. The effect on NBT reduction of DCH and MH subjected to BLIA for 0.5, 1, 1.5 and 2 h is shown in Fig. 7.

Fig. 7 shows that the photolytic effect of DCH or MH on NBT reduction was increased in an interval of 2 h under BLIA, suggesting that $O_2^{\bullet-}$ was generated from DCH or MH under BLIA in a time-dependent manner. The gradients of the NBT reaction curve for $O_2^{\bullet-}$ production due to DCH and MH that are subject to BLIA are 0.09 and 0.0261 (h^{-1}),

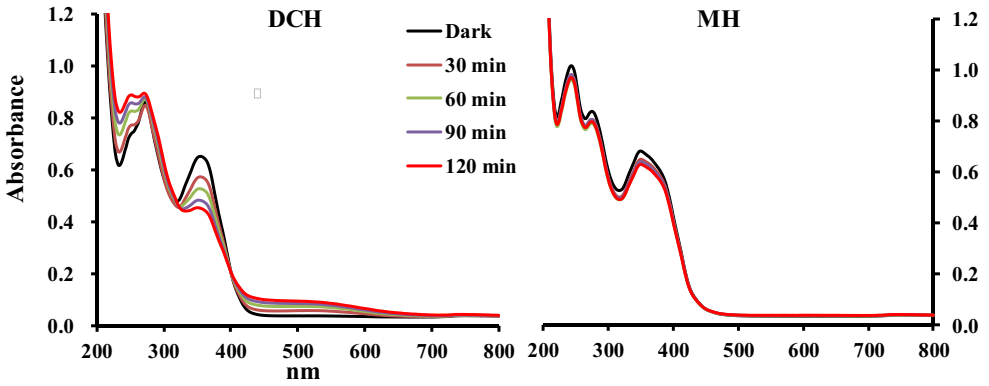

Fig. 5. Spectra for (A) DCH and (B) MH that were subjected to BLIA for 0.5–2 h.

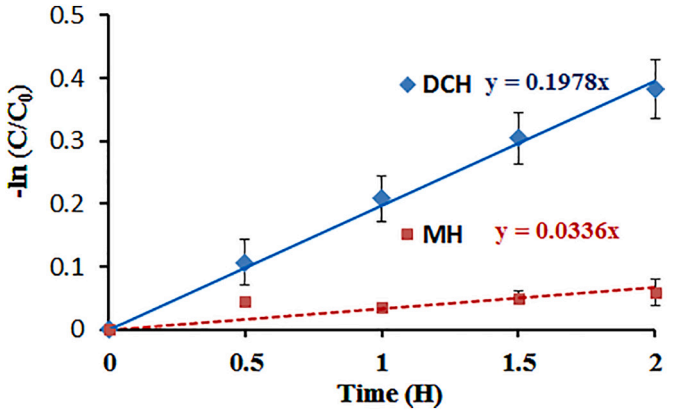

Fig. 6. Apparent decomposition rate constant, k_{appa}, for DCH and MH that are subjected to BLIA. Data are expressed as the mean ± SD, where $n = 3$.

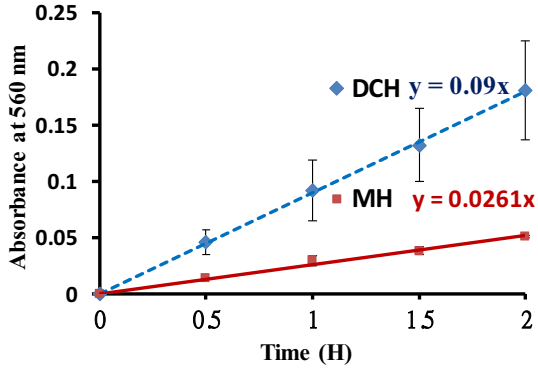

Fig. 7. Effects of DCH and MH subjected to BLIA on NBT reduction. Data are expressed as the mean ± SD, where $n = 3$.

respectively, as shown in Fig. 7.

3.3. Effects of DCH, MH and VAN that Are Subjected to BLIA on S. aureus and MRSA Viability

The effects of DCH, MH and VAN subjected to BLIA on *S. aureus* and MRSA/JD004 viability were determined in this study. Fig. 8A shows that there was no significant difference in the survivability of *S. aureus* in the presence of 0.1 mM DCH, 0.1 mM MH and 0.1 mM VAN in the dark. For DCH and MH that were subjected to BLIA for 2 h, there was a significant increase in the deactivation rate for *S. aureus*. The average suppressive effects of DCH and MH were subject to BLIA-induced inhibition of *S. aureus* by 3.84 and 1.65 log, respectively (Fig. 8B).

Fig. 9A shows that there was no significant difference in the survivability of MRSA/JD004 in the presence of 0.1 mM DCH, 0.1 mM MH and 0.1 mM VAN in the dark. For DCH and MH subjected to BLIA for 2 h, there was a significant increase in the deactivation rate for MRSA/JD004. The average suppressive effects of DCH and MH after BLIA treatment on the viability of MRSA/JD004 cells were 5.15 and 2.08 log, respectively (Fig. 9B).

3.4. $O_2^{\bullet-}$ Detection by DCH- or MH-Treated S. aureus that Are Subjected to BLIA

The generation of $O_2^{\bullet-}$ in *S. aureus* from DCH- or MH-treated *S. aureus* subjected to BLIA was determined using the NBT reduction method. As shown in Fig. 10, the absorbance at 560 nm of the NBT reaction for $O_2^{\bullet-}$ production in *S. aureus* due to treatment without or with DCH under BLIA is 0.093 or 0.50. However, Fig. 10 also shows that the photolytic effect of DCH-treated *S. aureus* on NBT reduction was increased under BLIA, suggesting that $O_2^{\bullet-}$ in *S. aureus* was abundantly generated.

3.5. Molecular Determination Using HPLC–MS Analysis

The structural change in DCH after illumination with blue light was investigated in this study. Exposure to BLIA for 2 h reduced 0.1 mM DCH and MH by 54.1 and 6.2% compared to its original compounds, respectively, based on a calculation from the HPLC–MS assay. As shown in Figs. 4, 5 and 6, DCH is photolytically sensitive while MH is relatively stable under BLIA.

The chromatograms of DCH before and after BLIA treatment are shown in Fig. 11. After DCH hydrolysis, doxycycline (DC) was eluted at 19.297 min and displayed a molecular ion m/z at 442.9 (Fig. 12C). The photochemical products of DCH (PPDs) were noted at 10.137 and 15.799 min (Fig. 11B). The MS spectra for PPD-1 and PDD-2 exhibited major ion signals at m/z 460.8 and 458.8, respectively, as shown in Fig. 12A and B.

4. Discussion

A photosensitizer enhances and catalyses the different bonds in a molecule via a photochemical reaction to produce ROS. Pathogenic bacteria can be deactivated by light illumination with suitable photosensitizers. In this study, the aPDI of *S. aureus* and MRSA/JD004 via BLIA-induced ROS from DCH or MH was determined.

He et al. reported that doxycycline photoactivated with UVA and demeclocycline with violet light and UVA deactivated both MRSA and *E. coli* [27]. We showed that riboflavin-5′-phosphate (FMN) photolysis

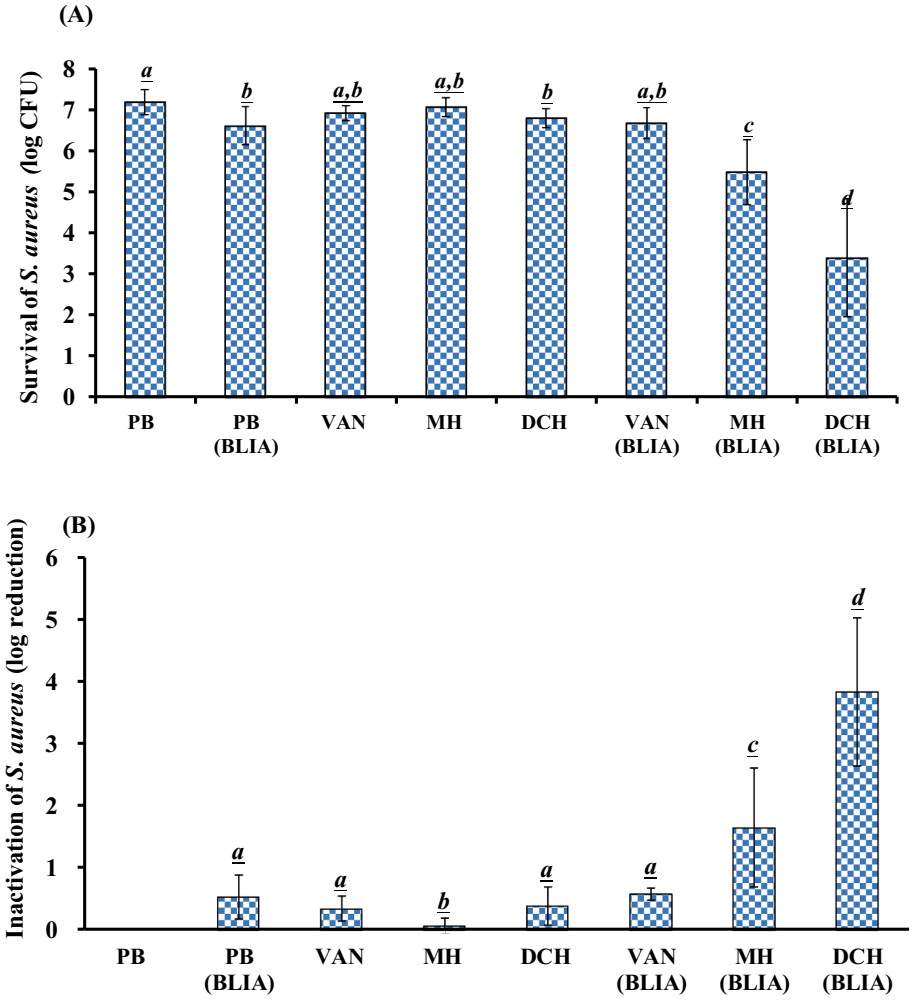

Fig. 8. Effects of the photolysis of DCH, MH and VAN that were subjected to BLIA for 2 h on the (A) viability and (B) deactivation rate of *S. aureus*. Data are expressed as the mean ± SD, where $n = 5$. Statistically significant differences ($p < 0.05$) between two groups are indicated by different letters above each bar.

under illumination by blue (λ = 465 nm) or violet light (λ = 405 nm) deactivates *S. aureus* and MRSA effectively [5]. Illumination with violet light in the presence of FMN is more effective for the deactivation of *S. aureus* than blue light at the same radiant intensity [5]. Wong et al. reported that with a shorter wavelength at violet light, the UV overlapping region can be risky to skin cells [5], while light with a longer wavelength is safer because it has a lower energy. Thus, the DCH-mediated blue light aPDI in this study may be safe.

TCs have been widely used to treat many skin conditions, such as infections, inflammation, or both. DCH and MH are often used to treat acne vulgaris [16]. In terms of the sensitivity to blue light illumination in PB at pH 7.8, DCH-based BLIA treatment produced more $O_2^{\bullet-}$ than the MH-based treatment. Currently, fluorescent lamps are being replaced by white LED lamps because LED lamps are more efficient. A white LED light source may be feasible for BLIA in aPDI. The spectrum of a white LED lamp comprises multiple colours of light, and the wavelengths of the major emitted maxima are 454 and 521 nm [18]. The efficiency with which $O_2^{\bullet-}$ is produced under white LED light via NBT reduction is approximately 75% of that using blue LED light [18].

As shown in Fig. 9B, in the absence of light exposure, DCH had negligible effects on MRSA/JD004 survival. Papkou et al. reported that the evolutionary resistance of *S. aureus* is related to the activity of the efflux pump [44], which can contribute to the intrinsic resistance of the bacteria towards antibiotics, such as ciprofloxacin [44–46]. The bactericidal agent should achieve the inhibition of bacterial growth at a rate of at least 3 log reduction [19]. As shown in Figs. 8 and 9, the DCH-treated photoreaction inhibited the growth of *S. aureus* and MRSA/JD004 by 3.84 and 5.15 log, respectively, while MH-based BLIA deactivated bacteria by less than 3 log. The DCH-treated photoreaction was found to be more efficient in *S. aureus* or MRSA/JD004 inactivation than the MH-treated photoreaction at the same radiant intensity. DCH is sensitive to blue light treatment, as evidenced by $O_2^{\bullet-}$, which is formed by a photolytic reaction of DCH under BLIA, as shown in Fig. 7. A previous study showed that the cleavage of both the supercoiled plasmid DNA of *E. coli* and genomic DNA of *S. aureus* can be induced by $O_2^{\bullet-}$ from FMN photolysis [5,18,21]. ROS from the photoreaction of FMN may either occur within cells or be conveyed from the outside by passing through membranes. Based on these observations, excessive DNA strand breakage was believed to be associated with the depletion of cellular ATP and NAD^+ levels, i.e., interference with ATP synthesis, which eventually led to cell death [47].

According to our previous study, for *S. aureus* under blue light (λ = 465 nm) illumination at 2.0 mW/cm^2 for 120 min (energy dose, 14.4 J/cm^2) and violet (λ = 405 nm) illumination at 1.0 mW/cm^2 for 20 min (energy dose, 1.2 J/cm^2), the inactivation rates were 26.3 and 27.1%, respectively [5]. The inactivation capacity of violet light was greater than that of blue light at the same radiant intensity [5]. Maclean et al. reported that wavelengths of irradiation longer than 430 nm without exogenous photosensitizer were ineffective in killing *S. aureus* cells, suggesting that endogenous porphyrins in *S. aureus* have a maximum inactivation at 405 ± 5 nm [48].

The viability of *S. aureus* and MRSA/JD004 under blue light (λ = 462

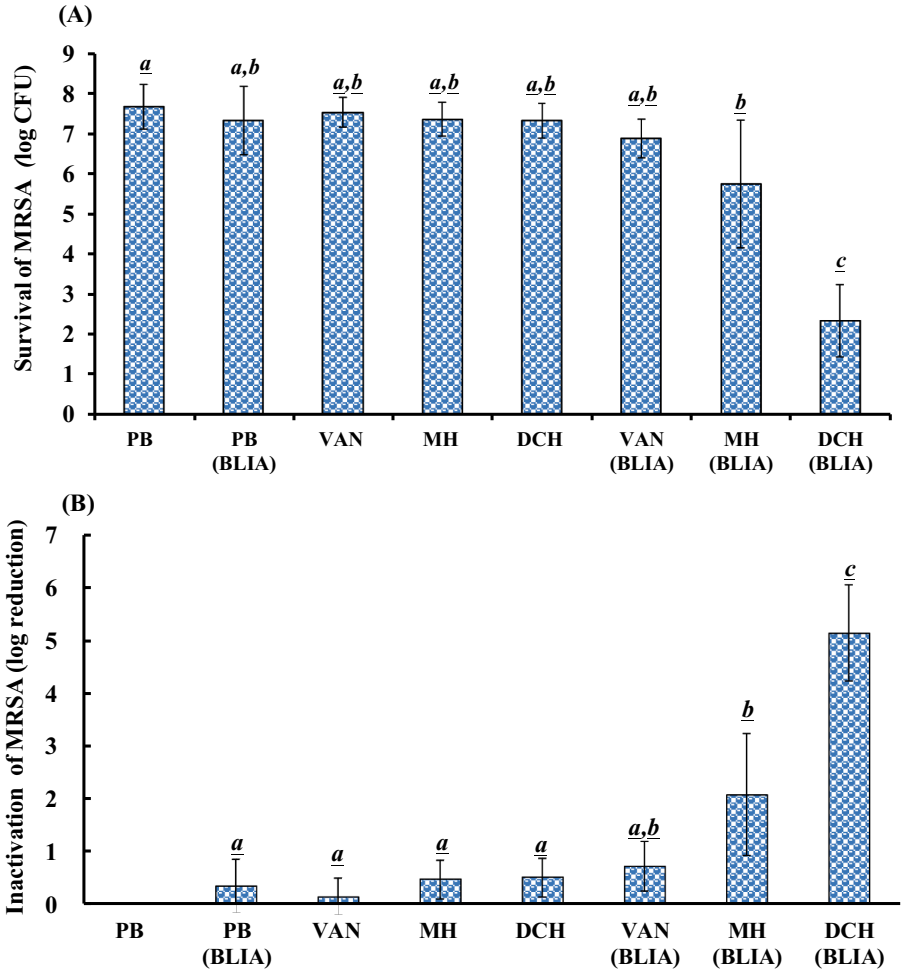

Fig. 9. Effects of the photolysis of DCH, MH and VAN subjected to BLIA for 2 h on the (A) viability and (B) deactivation rate of MRSA/JD004. Data are expressed as the mean ± SD, where $n = 4$. Statistically significant differences ($p < 0.05$) between two groups are indicated by different letters above each bar.

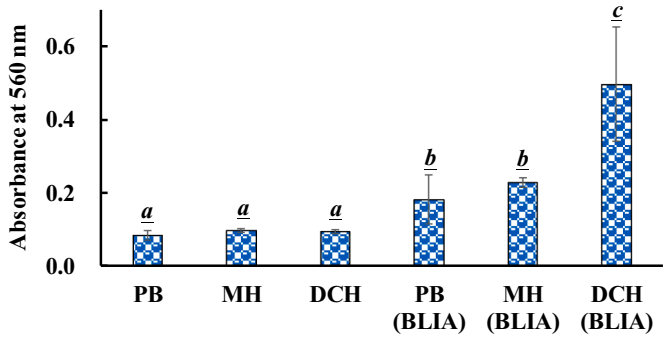

Fig. 10. Effects of DCH- or MH-treated *S. aureus* subjected to BLIA for 2 h on NBT reduction. Data are expressed as the mean ± SD, where n = 4. Statistically significant differences ($p < 0.05$) between two groups are indicated by different letters above each bar.

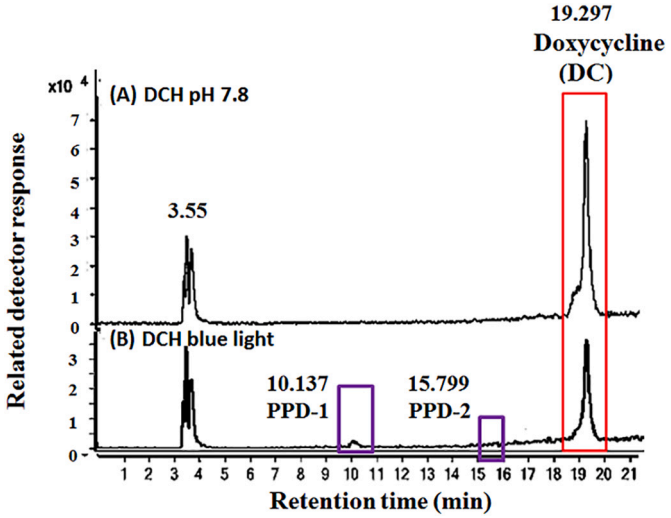

Fig. 11. Total ion chromatogram obtained via an HPLC–MS assay of (A) 0.1 mM DCH solution and (B) DCH that was subjected to BLIA for 2 h.

nm) illumination alone at 2.0 mW/cm^2 for 120 min (energy dose, 14.4 J/cm^2) was decreased by 0.54 (second bar, PB (BLIA), Fig. 8A) and 0.35 log (second bar, PB (BLIA), Fig. 9A), respectively. In Fig. 10, the level of $O_2^{\bullet-}$ produced in *S. aureus* subjected to BLIA is low, i.e., the effects of endogenous photosensitizers on the reduced viability of *S. aureus* under BLIA are quite minor compared to what occurred in the presence of DCH in this study. However, under the same conditions, DCH subjected to BLIA decreased the viability of *S. aureus* and MRSA/JD004 by 3.84 and 5.15 log, respectively. The generation of $O_2^{\bullet-}$ in DCH-treated *S. aureus* subjected to BLIA was extensively increased, as shown in Fig. 10. The strongly enhanced effects caused by exogeneous photosensitizers (DCH)

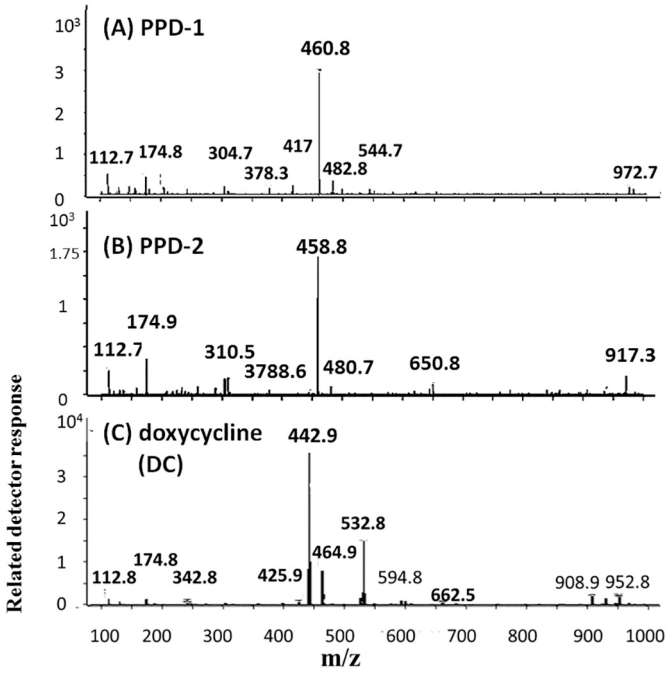

Fig. 12. Electron ionization mass spectra for DC and the PPDs from DCH that is subjected to BLIA: ion spectral products of $[M–H]^-$ are noted for DCH that is illuminated with blue light. The selected precursor ion is m/z 443, and the proposed fragments are shown. (For interpretation of the references to colour in this figure legend, the reader is referred to the web version of this article.)

on the inactivation of *S. aureus* and MRSA/JD004 under BLIA reach up to 3.3 and 4.8 log, respectively, and these values are much higher than those achieved by endogenous intracellular photosensitizers alone. These results bolster the finding that DCH under BLIA leads to enhanced deactivation of bacteria and has the potential to eradicate bacteria on a wound.

DCH-treated photoreaction significantly decreased the growth of both *S. aureus* and MRSA/JD004 examined in this study. Moreover, in terms of bacterial growth reduction, Souza et al. reported that MRSA strains were more susceptible to aPDI than methicillin-susceptible *Staphylococcus aureus* (MSSA) strains under low irradiation fluences [49]. During indocyanine green (ICG)-based aPDI (ICG-aPDI), the killing of the *S. aureus* resistant was achieved at lower amount of ICG compared to the bacterial effect observed in the wild-type *S. aureus* [50] The difference in the deactivation between resistant and wild-type strains of *S. aureus* is hypothetically due to variation of their outer layer structures in the binding or uptake of photosensitizers [51,52]. Additionally, MRSA might be more sensitive to the hydrolysis products of TC during and after irradiation, due to the lack of detectable PBP2a as no *mecA* expression was noticed in MRSA/JD004 after ICG-aPDI, making the bacteria more sensitive to oxacillin, cefoxitin, erythromycin, or tetracycline, which is partly related to *mecA* complex gene deletion [53]. In our previous study, TC-treated photoreaction inhibited the growth of *MDR E. coli* by 4 to 5 log, and the photolysis product of TC without light exposure could inactivate 30% MDR *E. coli* [30]. The photolytic product of TC increased the adversity risk to bacteria after BLIA. Tetracyclines therefore function as dual-action light-activated antibiotics by killing MRSA and *E. coli* in the presence of light and preventing their regrowth afterwards in the dark [27,54]. DCH-treated photoreaction inhibited MRSA/JD004 growth via ROS production in this study. After BLIA, MRSA/JD004 might become more sensitive to the treatment of both DCH and its photolysis product, which might bring a higher adversity risk to the bacteria.

TCs are phenolic compounds that are unstable and easily dissociate a proton to form a phenolate anion via an electron transfer mechanism in alkaline aqueous circumstances [55]. After photodegradation of the tetracycline antibiotics TC and chlortetracycline (CTC) under simulated sunlight, the quantum yields of direct photolysis increased from 3.4×10^{-4} to 1.1×10^{-2} and 3.3×10^{-4} to 8.5×10^{-3}, respectively, within the pH range of 6 to 9 [25,26].

The normal intact skin is acidic and has a pH value of 4.5–5.0. Shukla et al. reported the baseline pH of acute and chronic wounds, either infected or noninfected, in 50 patients from a single wound clinic, and most of the pH values were greater than 8.5. Only after the wound condition improved and exudate levels decreased did the pH decrease to less than 8.0 [56]. Elevated wound fluid pH was reported to correlate with an increased risk of wound infection. The mean pH value of infected wounds was 7.2 (pH 6–pH 9), which is higher than the mean pH of 6.5 in uninfected wounds [57]. The increase in pH value is proposed as a good indicator of local wound infection in second-degree burn wounds. The pH rose (turned alkaline) prior to the onset of clinical signs of local infection in 6 cases compared to 20 noninfected cases [30,58]. For the healing of skin wounds, the effects of pH on human primary keratinocyte and fibroblast functions show that both cell types tolerate a wide range of pH values very well (pH 5.5–9.5), although alkaline conditions significantly enhanced cell proliferation. Moreover, in vivo experiments in a rat full-thickness wound model indicated that a prolonged, strongly acidic environment prevents both wound closure and re-epithelialization while an alkaline environment did not have any negative impact [59]. DCH is a tetracycline antibiotic that is unstable under blue light illumination in alkaline aqueous conditions. As shown in Fig. 7, aerobic oxidative photolysis of DCH via BLIA generated a high level of $O_2^{\bullet-}$ and in turn decreased the viability of both *S. aureus* and MRSA/JD004 to a huge extent, suggesting that the aPDI of bacteria in the presence of exogeneous photosensitizers and light activation can be used to treat skin and soft tissue infections.

The different levels of photodegradation caused by BLIA between DCH and MH can be at least partially explained by their structural differences. Both DCH and MH share a linear fused tetracyclic nucleus (rings labelled A, B, C and D) that differs at positions five, six and seven of these two antibiotics, such as the dimethyl amino group attached to ring D of MH, as shown in Fig. 1. Assuming that the methyl group attached to ring C of DCH has little effect on the degradation process, the lower photosensitivity of MH is most likely due to its dimethyl amino group attached to ring D of MH, which does not exist in DCH. The effect of blue light illumination on amino phenol compounds, such as phenol, *o*-aminophenol, *m*-aminophenol, 3-dimethylaminophenol and *p*-aminophenol photolysis, has been determined. The spectra for phenol, *m*-aminophenol, 3-dimethylaminophenol and *p*-aminophenol in PB at pH 7.8 remained unchanged after BLIA treatment for 2 h, as shown in Fig. 13A, C, D and E. However, for *o*-aminophenol in PB with BLIA, the spectrum significantly differed from that of the dark control, as shown in Fig. 13B.

The hydroxyl group of ring D and carbonyl oxygen of ring C within both DCH and MH can form hexagonal intramolecular hydrogen bonds. The formation of intramolecular hydrogen bonds is tightly associated with the nonradiation intersystem crossing (ISC) process of aminofluorenones, i.e., $S_1 \leftrightarrow T_1$ states [60]. The ISC process occurs after photoexcitation, thus leading to the less favourable process phosphorescence and increasing the electronic agitation of the molecule. These changes are presumably followed by photodegradation of molecules that contain intramolecular hydrogen bonds, which was evidenced in *o*-aminophenol illuminated by blue light, but not phenolic compounds that are attached with *m*- or *p*-amino substituents or phenol alone, as shown in Fig. 13, suggesting the role of intramolecular hydrogen bonding in the degradation of phenolic compounds examined herein. For the low photosensitivity of MH, the dimethylamino group, a strong-electron donating group, of ring D in MH may donate electrons to the phenolic ring via a resonance effect. These changes increase the electronegative charge of the carbon atom of ring D by which −OH is attached, decrease the electronegativity of the oxygen atom of −OH,

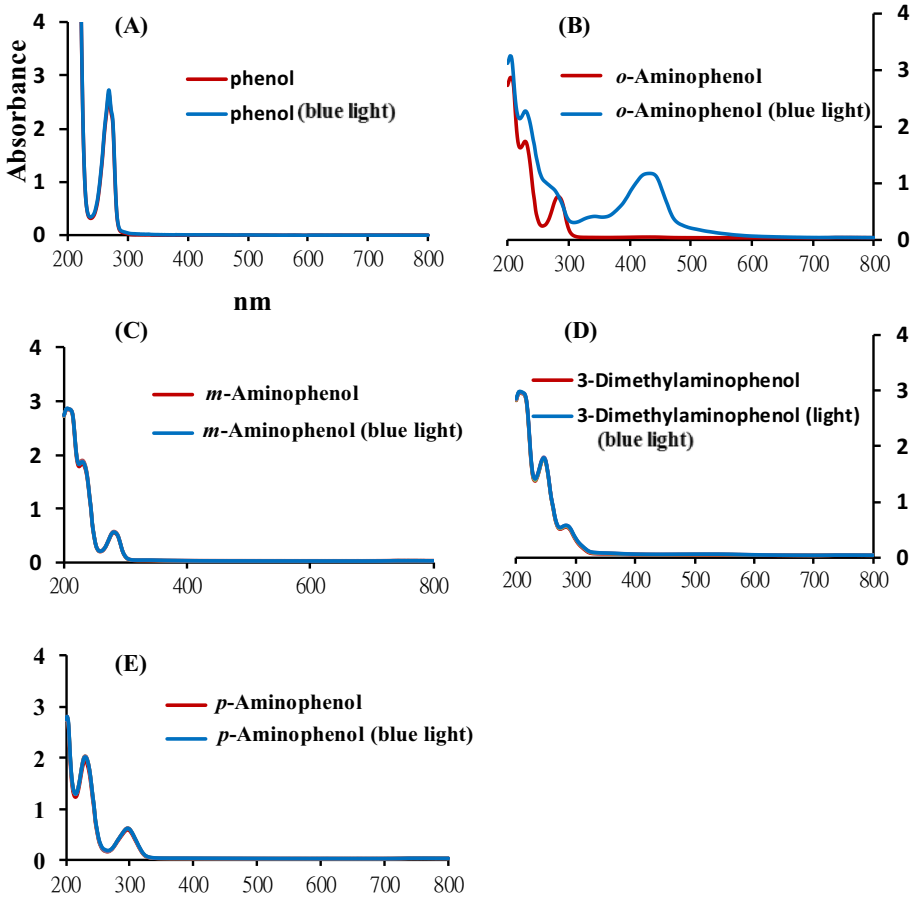

Fig. 13. Absorption spectra for (A) phenol, (B) *o*-aminophenol, (C) *m*-aminophenol, (D) 3-dimethylaminophenol and (E) *p*-aminophenol in PB at pH 7.8 with or without BLIA after 2 h.

likely decrease the exposure of the hydroxyl hydrogen nucleus, and weaken the intramolecular hydrogen bond between the carbonyl oxygen and the H atom of the −OH of ring C and D, respectively, thereby reducing the extent of high-energy ISC and decreasing the level of photodegradation in MH compared to what occurs in DCH.

According to previous results, several major pathways of DCH photodegradation are proposed, such as hydrolysis, photolysis, electron transfer, and production involving $O_2^{\bullet-}$ and •OH, as shown in Eqs. 3–6. The $O_2^{\bullet-}$ from the DCH photoreaction is important to the kinetics of DCH photodegradation. Chen et al. showed that $O_2^{\bullet-}$ was generated by photolysis of TC under illumination by simulated sunlight [25]. The superoxide anion radical $O_2^{\bullet-}$ disproportionally forms O_2 and H_2O_2, and H_2O_2 can be further decomposed to •OH by light illumination [61]. Liu et al. examined the •OH that occurs in an aqueous solution of oxytetracycline (OTC) under UV light illumination and concluded that oxygen can accept an electron to form $O_2^{\bullet-}$, which is reduced to yield H_2O_2 and then •OH [62]. The •OH radical species generated from the photolytic cleavage of the peroxidic bond in H_2O_2 can attack organic molecules [61]. The hydroxylation byproducts via dehydration from the OTC photoreaction can be generated in an aqueous OTC solution under UV light illumination [62]. Niu et al. also showed that TC directly reacts with $O_2^{\bullet-}$ in the photoreaction and undergoes self-sensitized photolysis mediated by $O_2^{\bullet-}$ [35]. The transformation products of TC exhibit evolution profiles in a time-dependent manner during TC photodegradation [63]. DCH is a tetracycline antibiotic that is unstable under blue light illumination in alkaline aqueous conditions. As shown in Fig. 7, the aerobic oxidative photolysis of DCH activated via illumination generated a high level of $O_2^{\bullet-}$. According to those previous results, several major pathways of DCH photodegradation are proposed and shown in the following equations.

$$DCH + O_2 + e^- \xrightarrow[\textit{hydrolysis}]{h\nu} DC^{\bullet+} + O_2^{\bullet-} \quad (3)$$

$$O_2^{\bullet-} + H^+ + e^- \xrightarrow{h\nu} HOO^{\bullet} \quad (4)$$

$$2\,HOO^{\bullet} + H_2O \rightarrow H_2O_2 + O_2 \quad (5)$$

$$H_2O_2 + e^- \xrightarrow{h\nu} 2\,{}^{\bullet}OH \quad (6)$$

Based on the results in this study, we also present the proposed mechanism of the DCH photoreaction under blue light illumination in Fig. 14. First, for the *N*-demethylation and two monohydroxylation processes shown in Fig. 7 and Eqs. (3)–(6), both $O_2^{\bullet-}$ and •OH could be formed by the photosensitized oxidation of DCH under blue light illumination. Doxycycline (DC) can be formed via DCH hydrolysis, as shown in Fig. 11. DC can achieve an electronically excited state, and then molecular oxygen can receive an electron from the excited DC, thus forming the N-centred amine radical cation of DC ($DC^{\bullet+}$) (Fig. 14C). Then, deprotonation ($-H^+$) of α-C led to the formation of a carbon-centred radical. The C-centred radical reacted rapidly with dissolved oxygen to produce a peroxyl radical species with further loss of a superoxide anion radical ($O_2^{\bullet-}$), which yields an iminium cation [64,65]. It is well known that imine is chemically unstable in aqueous solution and may undergo hydrolysis quickly to form the aforementioned *N*-demethylation product and an abundance of the characteristic compound D (*m/z* 429, $C_{21}H_{22}N_2O_8$) or 4-demethyldoxycycline (Fig. 14D). As an electrophilic species, •OH reactions primarily occur by hydrogen

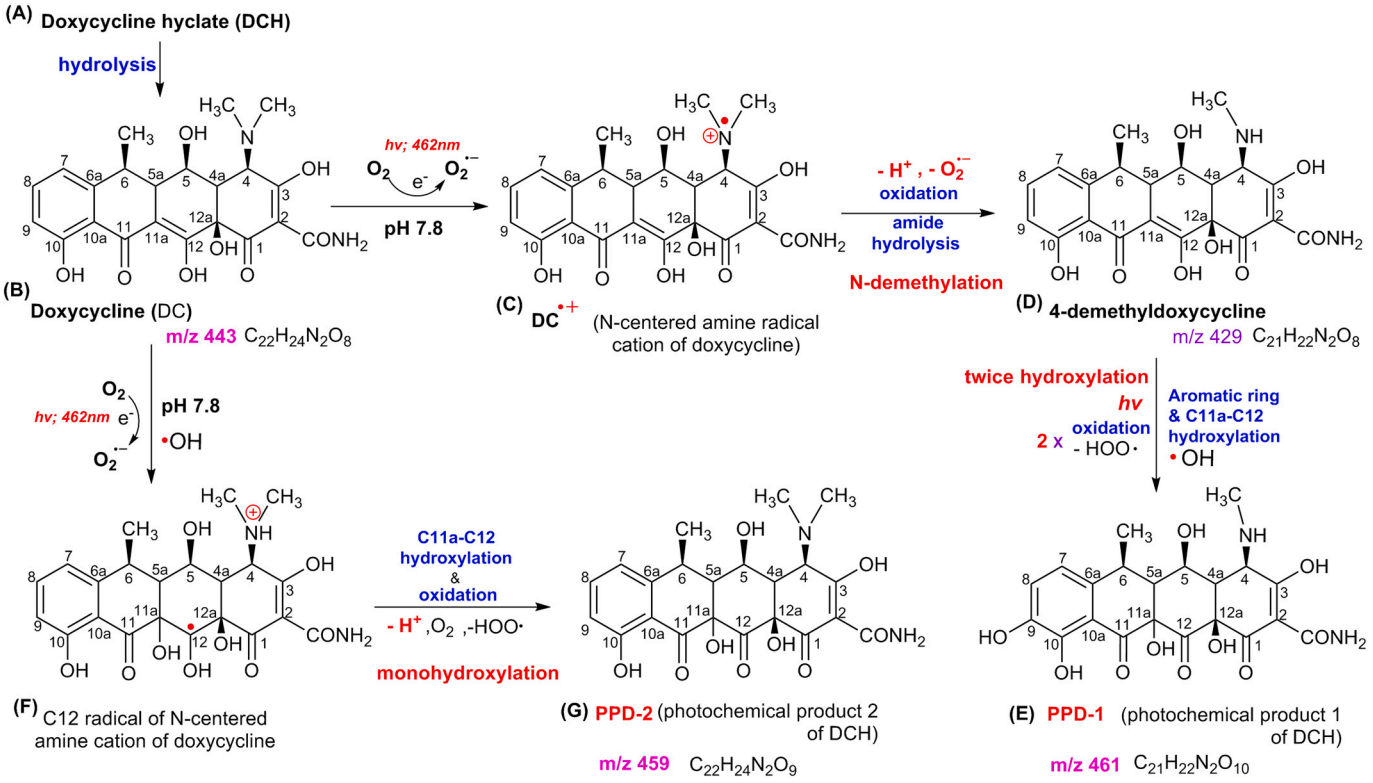

Fig. 14. Proposed scheme for DCH photolysis.
(A): Doxycycline hyclate (DCH); (B): doxycycline (DC); (C): N-centred amine radical cation of DC; (D): 4-demethyldoxycycline; (E): photochemical product 1 of DCH photolysis; (F): C12 radical of N-centred amine cation of doxycycline; and (G): photochemical product 2 of DCH photolysis.

abstraction, addition to a double bond and electron transfer [62]. C8-C9 of aromatic ring D and C11a–C12 of ring B are sensitive to diffusible •OH due to hydroxyl addition to these double bonds [62,66]. According to the light-induced autoreaction that formed the most characteristic molecular ions ($[M-H]^-$), i.e., m/z 461, and they correspond to byproduct PPD-1 ($C_{21}H_{22}N_2O_{10}$) formed via oxidation at C9 and C12 (Fig. 14E) [62,65]. Alternatively, •OH attacks the phenolic moiety of the doxycycline molecular structure (B ring), thus forming the C12 radical of the N-centred amine cation of DC (Fig. 14F) because the monohydroxylation process occurs at the C11a–C12 enolic double bond of ring B, which is sensitive to •OH addition [66]. Light-induced hydroxylation forms the most characteristic molecular ion ($[M-H]^-$), i.e., m/z 459, and it is attributed to the byproduct PPD-2 ($C_{22}H_{24}N_2O_9$) generated via oxidation of C12, as shown in Fig. 14G [30,35].

5. Conclusions

The effect of blue light irradiation on the viability of *Staphylococcus aureus* (*S. aureus*) and MRSA with doxycycline hyclate (DCH) and minocycline hydrochloride (MH) photolysis were studied. DCH is sensitive to blue light illumination, whereas MH is insensitive because of their structural difference. Chromatography results show that the chromogenic photolytic products of DCH are formed by blue light irradiation under alkaline conditions. DCH illuminated by blue light undergoes photolytic oxidation with a quantum yield of $O_2^{\bullet-}$ and increases the deactivation rate of *S. aureus* and MRSA due to ROS. The findings for antibacterial photodynamic deactivation of bacteria can be used to treat diseases, such as surface skin or deep subcutaneous infections, by installing an optical fibre to transfer blue light to the infected tissues.

Author Contributions

Experiment analysis, Sin He; investigation, Ji-Yuan Liang; methodology, Shiuh-Tsuen Huang and Tak-Wah Wong; project administration, Shwu-Yuan Lee and Chien-Wei Cheng; resources, Meei-Ju Yang and Tak-Wah Wong; validation, Jeu-Ming P. Yuann and Shiuh-Tsuen Huang; writing—review and editing, Jeu-Ming P. Yuann and Ji-Yuan Liang. All authors have read and agreed to the published version of the manuscript.

Declaration of competing interest

The authors declare no conflict of interest.

Acknowledgements

The authors are grateful to Dr. Chi-Ming Chiu, Mr. Ze-Yong Yang and Mr. Tang-Yu Chen for their assistance with the experimental works. The study was partly supported by Taiwan Ministry of Science and Technology MOST-109–2327-B-006–005, MOST 110–2314-B-006–086-MY3, and the Centre of Applied Nanomedicine, National Cheng Kung University from the Featured Areas Research Centre Programme within the framework of the Higher Education Sprout Project by the Ministry of Education (MOE) in Taiwan to TW Wong.

References

[1] I. Chopra, M. Roberts, Tetracycline antibiotics: mode of action, applications, molecular biology, and epidemiology of bacterial resistance, Microbiol. Rev. 65 (2001) 232–260.
[2] M.C. Roberts, Tetracycline resistance determinants: mechanisms of action, regulation of expression, genetic mobility, and distribution, FEMS Microbiol. Rev. 19 (1996) 1–24.
[3] N. Balaban, A. Rasooly, Staphylococcal enterotoxins, Int. J. Food Microbiol. 61 (2000) 1–10.
[4] A.F. Cardona, S.E. Wilson, Skin and soft-tissue infections: a critical review and the role of telavancin in their treatment, Clin. Infect. Dis. 61 (Suppl. 2) (2015) S69–S78.

[5] T.W. Wong, C.W. Cheng, Z.J. Hsieh, J.Y. Liang, Effects of blue or violet light on the inactivation of *Staphylococcus aureus* by riboflavin-5′-phosphate photolysis, J. Photochem. Photobiol. B Biol. 173 (2017) 672–680.

[6] A. Saeed, F. Ahsan, M. Nawaz, K. Iqbal, K.U. Rehman, T. Ijaz, Incidence of vancomycin resistant phenotype of the methicillin resistant *Staphylococcus aureus* isolated from a tertiary care hospital in Lahore, Antibiotics 9 (2019) 82.

[7] J.H. Lee, Methicillin (Oxacillin)-resistant *Staphylococcus aureus* strains isolated from major food animals and their potential transmission to humans, Appl. Environ. Microbiol. 69 (2003) 6489–6494.

[8] M. Barber, Methicillin-resistant staphylococci, J. Clin. Pathol. 14 (1961) 385–393.

[9] L.K. McDougal, C.D. Steward, G.E. Killgore, J.M. Chaitram, S.K. McAllister, F. C. Tenover, Pulsed-field gel electrophoresis typing of oxacillin-resistant *Staphylococcus aureus* isolates from the United States: establishing a national database, J. Clin. Microbiol. 41 (2003) 5113–5120.

[10] N.T. Nhung, C.T. Thuy, N.V. Trung, J. Campbell, S. Baker, G. Thwaites, N.T. Hoa, J. Carrique-Mas, Induction of antimicrobial resistance in *Escherichia coli* and non-typhoidal *Salmonella* strains after adaptation to disinfectant commonly used on farms in Vietnam, Antibiotics 4 (2015) 480–494.

[11] K. Hiramatsu, Vancomycin-resistant Staphylococcus aureus: a new model of antibiotic resistance, Lancet Infect. Dis. 1 (2001) 147–155.

[12] L.J. Xie, R.L. Wang, D. Wang, L. Liu, L. Cheng, Visible-light-mediated oxidative demethylation of N(6)-methyl adenines, J. Chem. Soc. Chem. Commun. 53 (2017) 10734–10737.

[13] M. Tim, Strategies to optimize photosensitizers for photodynamic inactivation of bacteria, J. Photochem. Photobiol. B Biol. 150 (2015) 2–10.

[14] T. Maisch, S. Hackbarth, J. Regensburger, A. Felgentrager, W. Baumler, M. Landthaler, B. Roder, Photodynamic inactivation of multi-resistant bacteria (PIB) - a new approach to treat superficial infections in the 21st century, J. Dtsch. Dermatol. Ges. 9 (2011) 360–366.

[15] M.R. Hamblin, Antimicrobial photodynamic inactivation: a bright new technique to kill resistant microbes, Curr. Opin. Microbiol. 33 (2016) 67–73.

[16] J.Q. Del Rosso, Oral doxycycline in the management of acne vulgaris: current perspectives on clinical use and recent findings with a new double-scored small tablet formulation, J. Clin. Aesthet Dermatol. 8 (2015) 19–26.

[17] T.W. Wong, E.C. Wu, W.C. Ko, C.C. Lee, L.I. Hor, I.H. Huang, Photodynamic inactivation of methicillin-resistant *Staphylococcus aureus* by indocyanine green and near infrared light, Dermatol. Sin. 36 (2018) 8–15.

[18] J.Y. Liang, C.W. Cheng, C.H. Yu, L.Y. Chen, Investigations of blue light-induced reactive oxygen species from flavin mononucleotide on inactivation of *E. coli*, J. Photochem. Photobiol. B Biol. 143 (2015) 82–88.

[19] M.J. Yang, Y.A. Hung, T.W. Wong, N.Y. Lee, J.M. Yuann, S.T. Huang, C.Y. Wu, I. Z. Chen, J.Y. Liang, Effects of blue-light-induced free radical formation from catechin hydrate on the inactivation of *Acinetobacter baumannii*, including a carbapenem-resistant strain, Molecules 23 (2018) 1631.

[20] J.M.P. Yuann, S.Y. Lee, M.J. Yang, S.T. Huang, C.W. Cheng, J.Y. Liang, A study of catechin photostability using photolytic processing, Processes 9 (2021) 293.

[21] J.Y. Liang, J.M. Yuann, C.W. Cheng, H.L. Jian, C.C. Lin, L.Y. Chen, Blue light induced free radicals from riboflavin on *E. coli* DNA damage, J. Photochem. Photobiol. B Biol. 119 (2013) 60–64.

[22] J.Y. Liang, J.P. Yuann, Z.J. Hsie, S.T. Huang, C.C. Chen, Blue light induced free radicals from riboflavin in degradation of crystal violet by microbial viability evaluation, J. Photochem. Photobiol. B Biol. 174 (2017) 355–363.

[23] T. Hasan, I.E. Kochevar, D.J. McAuliffe, B.S. Cooperman, D. Abdulah, Mechanism of tetracycline phototoxicity, J. Invest. Dermatol. 83 (1984) 179–183.

[24] I.M. Redelsperger, T. Taldone, E.R. Riedel, M.L. Lepherd, N.S. Lipman, F.R. Wolf, Stability of doxycycline in feed and water and minimal effective doses in tetracycline-inducible systems, J. Am. Assoc. Lab. Anim. Sci. 55 (2016) 467–474.

[25] Y. Chen, C. Hu, J. Qu, M. Yang, Photodegradation of tetracycline and formation of reactive oxygen species in aqueous tetracycline solution under simulated sunlight irradiation, J. Photochem. Photobiol. A Chem. 197 (2008) 81–87.

[26] Y. Chen, H. Li, Z. Wang, T. Tao, D. Wei, C. Hu, Photolysis of chlortetracycline in aqueous solution: kinetics, toxicity and products, J. Environ. Sci. 24 (2012) 254–260.

[27] Y. He, Y.Y. Huang, L. Xi, J.A. Gelfand, M.R. Hamblin, Tetracyclines function as dual-action light-activated antibiotics, PLoS One 13 (2018), e0196485.

[28] J.P. Martin Jr., K. Colina, N. Logsdon, Role of oxygen radicals in the phototoxicity of tetracyclines toward *Escherichia coli* B, J. Bacteriol. 169 (1987) 2516–2522.

[29] J.J. Huang, H.Y. Hu, Y.H. Wu, B. Wei, Y. Lu, Effect of chlorination and ultraviolet disinfection on tetA-mediated tetracycline resistance of *Escherichia coli*, Chemosphere 90 (2013) 2247–2253.

[30] S.T. Huang, C.Y. Wu, N.Y. Lee, C.W. Cheng, M.J. Yang, Y.A. Hung, T.W. Wong, J. Y. Liang, Effects of 462 nm light-emitting diode on the inactivation of *Escherichia coli* and a multidrug-resistant by tetracycline photoreaction, J. Clin. Med. 7 (2018) 278.

[31] Y.S. Lee, J.S. Yi, H.R. Lim, T.S. Kim, I.Y. Ahn, K. Ko, J. Kim, H.K. Park, S.J. Sohn, J. K. Lee, Phototoxicity evaluation of pharmaceutical substances with a reactive oxygen species assay using ultraviolet a, Toxicol. Res. 33 (2017) 43–48.

[32] W.P. Li, C.J. Yen, B.S. Wu, T.W. Wong, Recent advances in photodynamic therapy for deep-seated tumors with the aid of nanomedicine, Biomedicines 9 (2021) 69.

[33] M.A. Khan, J. Musarrat, Tetracycline–cu (II) photo-induced fragmentation of serum albumin, Comp. Biochem. Physiol. C Toxicol. Pharmacol. 131 (2002) 439–446.

[34] A.S. Li, H.P. Roethling, K.B. Cummings, C.F. Chignell, O_2− Photogenerated from aqueous solutions of tetracycline antibiotics (pH 7.3) as evidenced by DMPO spin trapping and cytochrome c reduction, Biochem. Biophys. Res. Commun. 146 (1987) 1191–1195.

[35] J. Niu, Y. Li, W. Wang, Light-source-dependent role of nitrate and humic acid in tetracycline photolysis: kinetics and mechanism, Chemosphere 92 (2013) 1423–1429.

[36] S. Miskoski, E. Sánchez, M. Garavano, M. López, A.T. Soltermann, N.A. Garcia, Singlet molecular oxygen-mediated photo-oxidation of tetracyclines: kinetics, mechanism and microbiological implications, J. Photochem. Photobiol. B Biol. 43 (1998) 164–171.

[37] S.T. Huang, Y.A. Hung, M.J. Yang, I.Z. Chen, J.P. Yuann, J.Y. Liang, Effects of epigallocatechin gallate on the stability of epicatechin in a photolytic process, Molecules 24 (2019).

[38] M.J. Yang, S.Y. Lee, C.I. Liu, S.H. Chen, I.Z. Chen, T.C. Su, J.M.P. Yuann, C. W. Cheng, S.T. Huang, J.Y. Liang, Catechin photolysis suppression by aluminum chloride under alkaline conditions and assessment with liquid chromatography–mass spectrometry, Molecules 25 (2020) 5985.

[39] R.E. Gavilan, C. Nebot, M. Veiga-Gomez, P. Roca-Saavedra, B. Vazquez Belda, C. M. Franco, A. Cepeda, A confirmatory method based on HPLC-MS/MS for the detection and quantification of residue of tetracyclines in nonmedicated feed, J. Anal. Methods Chem. 2016 (2016) 1202954.

[40] S.T. Huang, S.Y. Lee, S.H. Wang, C.Y. Wu, J.P. Yuann, S. He, C.W. Cheng, J. Y. Liang, The influence of the degradation of tetracycline by free radicals from riboflavin-5′-phosphate photolysis on microbial viability, Microorganisms 7 (2019) 500.

[41] C.W. Cheng, L.Y. Chen, C.W. Chou, J.Y. Liang, Investigations of riboflavin photolysis via coloured light in the nitro blue tetrazolium assay for superoxide dismutase activity, J. Photochem. Photobiol. B Biol. 148 (2015) 262–267.

[42] T. Ajiboye, A. Mohammed, S. Bello, I. Yusuf, O. Ibitoye, H. Muritala, I. Onajobi, Antibacterial activity of *Syzygium aromaticum* seed: studies on oxidative stress biomarkers and membrane permeability, Microb. Pathog. 95 (2016) 208–215.

[43] M. Becerra, I. Albesa, Oxidative stress induced by ciprofloxacin in *Staphylococcus aureus*, Biochem. Biophys. Res. Commun. 297 (2002) 1003–1007.

[44] A. Papkou, J. Hedge, N. Kapel, B. Young, R.C. MacLean, Efflux pump activity potentiates the evolution of antibiotic resistance across *S. aureus* isolates, Nat. Commun. 11 (2020) 3970.

[45] G.W. Kaatz, S.M. Seo, C.A. Ruble, Efflux-mediated fluoroquinolone resistance in *Staphylococcus aureus*, Antimicrob. Agents Chemother. 37 (1993) 1086–1094.

[46] K. Ubukata, N. Itoh-Yamashita, M. Konno, Cloning and expression of the norA gene for fluoroquinolone resistance in *Staphylococcus aureus*, Antimicrob. Agents Chemother. 33 (1989) 1535–1539.

[47] J.M.C.G. Barry Halliwell, Oxidative Stress: Adaptation, Damage, Repair and Death, in: Free Radicals in Biology and Medicine, Oxford University Press Inc., New York, 2003, pp. 246–350.

[48] M. Maclean, S.J. MacGregor, J.G. Anderson, G. Woolsey, High-intensity narrow-spectrum light inactivation and wavelength sensitivity of *Staphylococcus aureus*, FEMS Microbiol. Lett. 285 (2008) 227–232.

[49] B.M.N. Souza, J.G. Pinto, A.H.C. Pereira, A.G. Miñán, J. Ferreira-Strixino, Efficiency of antimicrobial photodynamic therapy with photodithazine® on MSSA and MRSA strains, Antibiotics 10 (2021) 869.

[50] N. Topaloglu, M. Gulsoy, S. Yuksel, Antimicrobial photodynamic therapy of resistant bacterial strains by indocyanine green and 809-nm diode laser, Photomed. Laser Surg. 31 (2013) 155–162.

[51] M. Grinholc, B. Szramka, J. Kurlenda, A. Graczyk, K.P. Bielawski, Bactericidal effect of photodynamic inactivation against methicillin-resistant and methicillin-susceptible *Staphylococcus aureus* is strain-dependent, J. Photochem. Photobiol. B Biol. 90 (2008) 57–63.

[52] H.M. Tang, M.R. Hamblin, C.M. Yow, A comparative in vitro photoinactivation study of clinical isolates of multidrug-resistant pathogens, J. Infect. Chemother. 13 (2007) 87–91.

[53] T.W. Wong, S.Z. Liao, W.C. Ko, C.J. Wu, S.B. Wu, Y.C. Chuang, I. Huang, Indocyanine green—mediated photodynamic therapy reduces methicillin-resistant *Staphylococcus aureus* drug resistance, J. Clin. Med. 8 (2019) 411.

[54] Q. Zhang, L. Jiang, J. Wang, Y. Zhu, Y. Pu, W. Dai, Photocatalytic degradation of tetracycline antibiotics using three-dimensional network structure perylene diimide supramolecular organic photocatalyst under visible-light irradiation, Appl. Catal. B 277 (2020), 119122.

[55] L.Y. Chen, C.W. Cheng, J.Y. Liang, Effect of esterification condensation on the Folin-Ciocalteu method for the quantitative measurement of total phenols, Food Chem. 170 (2015) 10–15.

[56] V. Shukla, D. Shukla, S. Tiwary, S. Agrawal, A. Rastogi, Evaluation of pH measurement as a method of wound assessment, J. Wound Care 16 (2007) 291–294.

[57] D.G. Metcalf, M. Haalboom, P.G. Bowler, C. Gamerith, E. Sigl, A. Heinzle, M.W. M. Burnet, Elevated wound fluid pH correlates with increased risk of wound infection, Wound Med. 26 (2019), 100166.

[58] S. Ono, R. Imai, Y. Ida, D. Shibata, T. Komiya, H. Matsumura, Increased wound pH as an indicator of local wound infection in second degree burns, Burns 41 (2015) 820–824.

[59] C.R. Kruse, M. Singh, S. Targosinski, I. Sinha, J.A. Sørensen, E. Eriksson, K. Nuutila, The effect of pH on cell viability, cell migration, cell proliferation, wound closure, and wound reepithelialization: in vitro and in vivo study, Wound Repair Regen. 25 (2017) 260–269.

[60] G.J. Zhao, K.L. Han, Role of intramolecular and intermolecular hydrogen bonding in both singlet and triplet excited states of aminofluorenones on internal conversion, intersystem crossing, and twisted intramolecular charge transfer, J. Phys. Chem. A 113 (2009) 14329–14335.

[61] C. Li, N. Gao, L. Wang, Y. Shen, Hydrogen peroxide-assisted low pressure UV photodegradation of atrazine in aqueous solution, J. Environ. Stud. 69 (2012) 625–634.
[62] Y. Liu, X. He, Y. Fu, D.D. Dionysiou, Degradation kinetics and mechanism of oxytetracycline by hydroxyl radical-based advanced oxidation processes, Chem. Eng. J. 284 (2016) 1317–1327.
[63] S. Li, J. Hu, Photolytic and photocatalytic degradation of tetracycline: effect of humic acid on degradation kinetics and mechanisms, J. Hazard. Mater. 318 (2016) 134–144.
[64] X. He, A.A. de la Cruz, A. Hiskia, T. Kaloudis, K. O'Shea, D.D. Dionysiou, Destruction of microcystins (cyanotoxins) by UV-254 nm-based direct photolysis and advanced oxidation processes (AOPs): influence of variable amino acids on the degradation kinetics and reaction mechanisms, Water Res. 74 (2015) 227–238.
[65] Y. Ji, Y. Shi, W. Dong, X. Wen, M. Jiang, J. Lu, Thermo-activated persulfate oxidation system for tetracycline antibiotics degradation in aqueous solution, Chem. Eng. J. 298 (2016) 225–233.
[66] R. Broszkiewicz, T. Söylemez, D. Schulte-Frohlinde, Reactions of OH radicals with acetylacetone in aqueous solution. A pulse radiolysis and electron spin resonance study, Z. Naturforsch. B 37 (1982) 368–375.